Theory of Fishnet Negative-Index Optical Metamaterials

J. Yang,[1] C. Sauvan,[1,2,*] H. T. Liu,[3] and P. Lalanne[1,2]

[1]*Laboratoire Charles Fabry de l'Institut d'Optique, CNRS, Université Paris Sud, Campus Polytechnique, RD128, 91127 Palaiseau, France*

[2]*Laboratoire Photonique Numérique et Nanosciences, Université Bordeaux, Institut d'Optique, CNRS, 33405 Talence, France*

[3]*Key Laboratory of Opto-electronic Information Science and Technology, Ministry of Education, Institute of Modern Optics, Nankai University, Tianjin 300071, China*

(Received 15 February 2011; revised manuscript received 11 June 2011; published 19 July 2011)

We theoretically study fishnet metamaterials at optical frequencies. In contrast with earlier works, we provide a microscopic description by tracking the transversal and longitudinal flows of energy through the fishnet mesh composed of intersecting subwavelength plasmonic waveguides. The analysis is supported by a semianalytical model based on surface-plasmon coupled-mode equations, which provides accurate formulas for the fishnet refractive index, including the real-negative and imaginary parts. The model simply explains how the surface plasmons couple at the waveguide intersections, and it shines new light on the fishnet negative-index paradigm at optical frequencies. Extension of the theory for loss-compensated metamaterials with gain media is also presented.

DOI: 10.1103/PhysRevLett.107.043903 PACS numbers: 42.25.Bs, 73.20.Mf, 78.20.Ci, 78.67.Pt

In the recently emerging fields of metamaterials and transformation optics, the possibility of creating optical negative-index metamaterials (NIMs) using nanostructured metal-dielectric composites has triggered intense basic and applied research over the past several years [1–4]. In view of potential applications of such structures in a variety of areas ranging from subwavelength imaging [1] to cloaking [5], it is important to understand the underlying physics in detail. Until now, our common understanding of optical NIMs was entirely based on the concept of homogenization. Different techniques have been developed, including field averaging [6], Bloch-mode computation [7–9], multipole expansion [10,11], and inversion of scattering parameters [12], all of them being based on fully vectorial electromagnetic calculations of the whole structure. Thus, even if these approaches quantitatively predict the light transport, they are often nonintuitive, thereby hindering the design process required to apply metamaterials into new optical technologies. At microwave frequencies, lumped-elements circuit models provide a reliable framework for understanding and designing the properties of NIMs [13,14]. Unfortunately, such a framework is lacking in the optical domain.

In this Letter, we study fishnet NIMs [3,4,7–9] by adopting a "microscopic" point of view. We abandon classical homogenization approaches, and instead we track the energy as it propagates and scatters through the fishnet mesh, like a fluid flowing in a multichannel system. The dynamics involves two intersecting subwavelength channels and their coupling; see Fig. 1. The longitudinal (z-direction) channel consists of air holes in a metal film, and the transversal (x-direction) channel is formed by metal-insulator-metal (MIM) waveguides that support the propagation of surface-plasmon polariton modes called gap-SPPs. Through simple equations that describe how both channels couple and exchange energy, we derive semianalytical formulas for the refractive index and the losses, and we explain how low-loss and negative values appear. The model can be seen as an extension of the lumped-elements models used in microwaves; the extension encompasses the treatment of Ohmic losses that limit the operation at high frequency and the abandonment of periodic conditions in the transversal direction [14]. The latter allows for an analytical treatment of the key parameters impacting the transversal gap-SPP resonance, which shines new light on the physical origin of negative refraction in fishnets. In particular, we evidence that the reduction of the gap-SPP damping constitutes the main

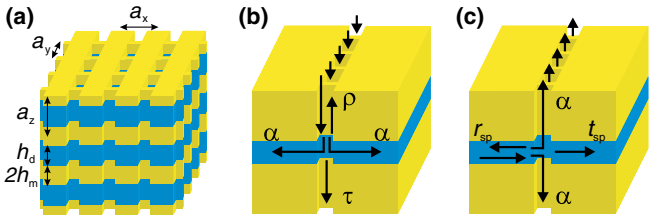

FIG. 1 (color online). Elementary scattering events in a fishnet. (a) The fishnet is a 2D array (period $a_x = a_y = 860$ nm) of rectangular holes (width $w_x = 295$ nm and $w_y = 595$ nm) etched into a Ag($h_m = 50$ nm)-MgF_2($h_d = 50$ nm)-Ag($h_m = 50$ nm) periodic stack. The refractive index of MgF_2 is $n_d = 1.38$, and the dispersive permittivity of silver is taken from Ref. [24]. (b) Scattering of the supermode of a 1D hole chain. (c) Scattering of the gap-SPP mode supported by a MIM waveguide. The scattering events in (b) and (c) define five elementary scattering coefficients: the reflection ρ and transmission τ of the supermode, the reflection r_{sp} and transmission t_{sp} of the gap-SPP, and the coupling coefficient α.

ingredient for the problem of loss compensation with gain media, a vital issue for NIMs in the visible and near-infrared [2,15–17].

It is worth emphasizing that all the salient properties of a fishnet are driven by its fundamental Bloch mode. Indeed, the negative refraction deduced from prism-deviation measurements can be explained by considering Snell's law at an interface between air and an effective medium with a refractive index equal to the effective index n_{eff} of the fundamental Bloch mode [4]. This observation has been recently confirmed by numerical results showing that the reflectance and the transmittance of finite-thickness fishnet slabs can be perfectly calculated by assuming that the energy transport inside the fishnet is solely due to the fundamental Bloch mode [9]. Therefore, the following analysis will be mainly devoted to understanding the origin of the negative n_{eff} values. The latter have been calculated with a Fourier Bloch-mode method [9] at normal incidence for the geometrical parameters used in Ref. [4] and given in the caption of Fig. 1. The simulation results (circles in Fig. 2) predict a negative-index band for $\lambda > 1.7$ μm, with low loss around 1.8 μm.

In order to understand these important features, we model the energy transport in the fishnet mesh as resulting from the flow of surface plasmons through two intersecting subwavelength channels. Both channels, along with the definition of the associated scattering coefficients, are depicted in Fig. 1. The longitudinal channel consists of a one-dimensional (1D) hole chain in a metal film; it supports the propagation of the supermode formed by the in-phase superposition of the TE_{01} modes of every hole. At the hole-chain boundaries, the supermode is partly transmitted (coefficient τ), reflected (coefficient ρ), or scattered (coefficient α) into the gap-SPP mode of the transversal MIM channel; see Fig. 1(b). Similarly, an incident gap-SPP is scattered by the hole chain; see Fig. 1(c). Because of Lorentz reciprocity theorem, the transversal scattering process defines only two additional coefficients denoted by r_{sp} and t_{sp}. Starting from the sole knowledge of the scattering coefficients ρ, τ, α, r_{sp}, and t_{sp} (calculated with a fully vectorial modal method [18]), we now provide a step-by-step analysis that brings us to derive an analytical expression for n_{eff}.

We first consider the elementary building block of the fishnet, the hole chain depicted in the inset (i1) of Fig. 2. The effective index n_h of its fundamental supermode is shown with dashed-dotted curves. The mode is evanescent at long wavelengths; $\mathrm{Im}(n_h)$ rapidly increases as the wavelength exceeds the cutoff at 1.4 μm, while $\mathrm{Re}(n_h)$ remains nearly null. Note that the spectral range of evanescence coincides with that of negative index [14,19].

We next consider a more involved structure: a single hole chain etched into a Ag-MgF_2-Ag periodic stack; see Fig. 2(i2). The Bloch mode of the z-periodic hole chain can be analytically derived by assuming that the field in the metallic holes is formed only by the superposition of two

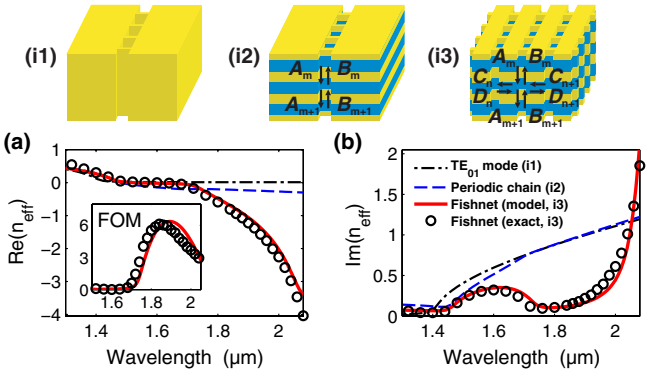

FIG. 2 (color online). Model predictions for (a) the real part and (b) the imaginary part of the effective index. We study successively with the model the supermode of a 1D hole chain [inset (i1), dashed-dotted black curves], the Bloch mode of a single z-periodic chain [inset (i2), dashed blue curves], and the Bloch mode of the fishnet [inset (i3), red curves]. Results of fully vectorial calculations are marked with circles. The figure of merit $|\mathrm{Re}(n_{\mathrm{eff}})|/\mathrm{Im}(n_{\mathrm{eff}})$ is shown in the inset of (a).

counterpropagating supermodes, a legitimate assumption for tiny holes. The transfer matrix that links the amplitudes of the forward and backward supermodes, A_m and B_m in Fig. 2(i2), is a 2×2 matrix: $A_{m+1} = \tau\upsilon A_m + \rho\upsilon B_{m+1}$ and $B_m = \rho\upsilon A_m + \tau\upsilon B_{m+1}$, where $\upsilon = \exp(ik_0 n_h a_z)$, a_z is the longitudinal period, and $k_0 = 2\pi/\lambda$. The Bloch-mode effective index n_{pc} is easily derived from the matrix eigenvalues [20], and one gets

$$\cos(k_0 n_{\mathrm{pc}} a_z) = \frac{\tau^2\upsilon^2 - \rho^2\upsilon^2 + 1}{2\tau\upsilon}. \qquad (1)$$

The longitudinal periodic structuring profoundly affects the nature of the energy transport [21], and, for wavelengths larger than the TE_{01} mode cutoff, n_{pc} is negative (dashed blue curves), an effect that we attribute to the launching of gap-SPPs into the transversal MIM waveguides. However, since $|\mathrm{Re}(n_{\mathrm{pc}})| \ll |\mathrm{Re}(n_{\mathrm{eff}})|$ and $\mathrm{Im}(n_{\mathrm{pc}}) \gg \mathrm{Im}(n_{\mathrm{eff}})$, the longitudinal structuring cannot alone explain the low-loss negative index of the fishnet. This reveals the importance of another effect, namely, a transversal resonant coupling that strengthens the gap-SPP excitation and that enables the appearance of large negative n_{eff} values.

We finally consider the whole fishnet, which can be viewed as an array of z-periodic hole chains that interact through the excitation of gap-SPPs. A closed-form expression for the fishnet effective index n_{eff} can be analytically derived by assuming that the energy transfer in the dielectric gaps is solely mediated by the fundamental gap-SPP mode with a symmetric magnetic field $H_y(-z) = H_y(z)$. Using the scattering coefficients r_{sp}, t_{sp}, and α, we easily derive additional coupled-mode equations for the gap-SPP amplitudes C_n and D_n defined in Fig. 2(i3). With the periodicity condition along x, we eliminate the C_n's and D_n's to obtain a new 2×2 matrix, where the scattering

coefficients ρ and τ have been replaced by $\rho + \gamma$ and $\tau + \gamma$ [20]. After diagonalization, we obtain the fishnet effective index n_{eff}:

$$\cos(k_0 n_{\text{eff}} a_z) = \frac{(\tau+\gamma)^2 v^2 - (\rho+\gamma)^2 v^2 + 1}{2(\tau+\gamma)v}, \quad (2)$$

with $\gamma = 2\alpha^2 u/[1-(t_{\text{sp}}+r_{\text{sp}})u]$, where $u = \exp(ik_0 n_{\text{sp}} a_x)$ is the gap-SPP phase delay over one period and $k_0 n_{\text{sp}}$ is the gap-SPP propagation constant. The transversal coupling between the hole chains is fully described by a single parameter γ, which physically represents the multiple scattering of the gap-SPPs in the MIM layers. The model predictions for the fishnet effective index are shown with the solid red curves in Fig. 2. They are found to quantitatively capture all the major features of the calculated data (circles), such as the negative n_{eff} for $\lambda > 1.7$ μm, the increase (in absolute value) of $\text{Re}(n_{\text{eff}})$ with the wavelength, and the low-loss band for $1.8 < \lambda < 2$ μm followed by a rapid increase of the loss at longer wavelengths. Even the band gap for $1.45 < \lambda < 1.7$ μm is accurately predicted. We have checked that the model accuracy is mainly limited by our assumption that the energy transfer through the metallic holes is solely due to the TE_{01} mode [20].

The main force of the model is to explicitly dissociate longitudinal and transversal contributions. The dispersion curve of a single z-periodic hole chain [Eq. (1) and dashed curves in Fig. 2] reflects only the longitudinal contribution and shows a large attenuation with a negligible negative index. Thus the transversal coupling mediated by gap-SPPs [described by the multiple-scattering parameter γ in Eq. (2)] clearly appears as the origin for the appearance of large negative n_{eff} values with low loss. The reduction of the attenuation, $\text{Im}(n_{\text{eff}}) \ll \text{Im}(n_{\text{pc}})$, is understood as follows: The gap-SPPs, which leak away in the case of a single hole chain, are recycled back into nearby chains in the fishnet. The increase (in absolute value) of $\text{Re}(n_{\text{eff}})$ is more delicate to analyze; it is due to a transversal resonance at $\lambda \approx 2$ μm that boosts the excitation of gap-SPPs and thus enhances the negativity that was only emerging in the hole chain. Figure 3(a) shows the Lorentzian shape of $|\gamma|^2$, which corresponds to the resonance of a periodic MIM waveguide coupled to two 2D arrays of semi-infinite vertical holes; see the inset. This resonance reflects into an enhancement of the gap-SPP field in the fishnet, as shown by the red curve in Fig. 3(b), which shows the normalized gap-SPP intensity $|C_n/A_m|^2$ ($D_n = C_n$ for normal incidence). The model predicts that $|C_n/A_m|^2$ increases by a factor of 10 as the wavelength varies from 1.7 to 2 μm, where a maximum is reached. This prediction is found to be in good agreement with fully vectorial computations (circles) and quantitatively supports the usual understanding that attributes the "magnetic" response of fishnets to an antisymmetric current distribution in the MIM stack [1,4,19,22]. Additionally, the model allows us to calculate

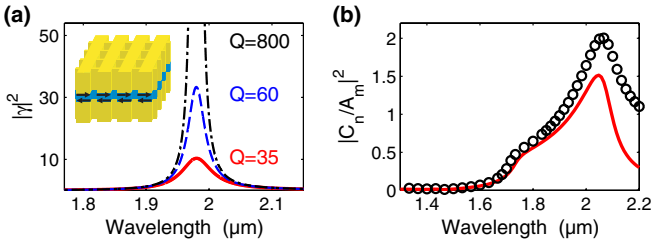

FIG. 3 (color online). Transversal gap-SPP resonance. (a) Impact of the gain g on the resonance of $|\gamma|^2$, $g = 0$ (solid red line), $g = 0.01$ (dashed blue line), and $g = 0.022$ (dashed-dotted black line). Inset: Periodic MIM waveguide perforated by semi-infinite metallic holes. (b) Normalized gap-SPP intensity $|C_n/A_m|^2$ in the fishnet. Good agreement is achieved between the model predictions (red curve) and the values extracted from a fully vectorial calculation of the fishnet Bloch mode (circles).

the $1/e^2$ decay length of the gap-SPP resonance, which is found to be delocalized over 4 periods.

Because of its analytical treatment, the model constitutes a powerful tool to design fishnets. We have stressed the major impact of the transversal resonance, both on the negative index and on the attenuation, and the dependence of the resonance position and lifetime on various parameters can be easily deduced from Eq. (2). The resonance spectral position can be tuned by controlling the gap-SPP phase-delay u, i.e., the period a_x or the dielectric refractive index. The model can also comprehensively address the loss limitation issue. Since $|r_{\text{sp}} + t_{\text{sp}}| \approx 1$ in the denominator of γ, the quality factor Q of the resonance is limited by the gap-SPP damping: $Q \approx \text{Re}(n_{\text{sp}})/[2\text{Im}(n_{\text{sp}})]$. It weakly depends on the geometry and can be mainly controlled by the choice of the materials.

A different approach to reduce losses is to incorporate active gain materials, and this issue has recently received much attention [15–17]. We start by considering the impact of gain on the resonance lifetime of γ. Numerical calculations have confirmed that the scattering coefficients in Eq. (2) (α, r_{sp}, t_{sp}, ρ, and τ) weakly depend on gain, and since v is unaffected (we incorporate gain only in the MgF_2 layers), gain is mainly impacting the gap-SPP propagation constant $k_0 n_{\text{sp}}$. Thus, the intricate problem of loss compensation in a fishnet metamaterial essentially reduces to a much simpler problem of loss compensation in a MIM waveguide. Hereafter we restrict the study to the low-loss band $1.75 < \lambda < 1.9$ μm, and we assume that the amplification process can be simply analyzed by a phenomenological refractive index $n_d = 1.38 - ig$ with a constant negative imaginary part. Consistently with previous studies [15–17], we choose $0 < g < 0.02$. These values are small enough to ensure a linear operation for which self-consistent calculations are not strictly required [16]. As anticipated, due to the decrease of the gap-SPP damping [see Fig. 4(a)], the transversal resonance is strengthened in the presence of gain, and the Q factor rapidly increases

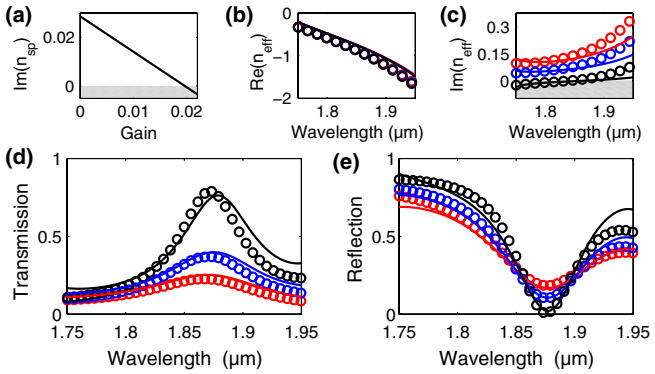

FIG. 4 (color online). Loss compensation with gain. (a) Decrease of the gap-SPP damping with the gain g ($\lambda = 1.9\ \mu$m). Amplified gap-SPPs are obtained in the gray region. (b),(c) Fishnet n_{eff} for three gain values: $g = 0$ (red line), 0.01 (blue line), and 0.022 (black line). (d),(e) Transmission and reflection spectra of a finite-thickness ($d = 5a_z$) fishnet for the same gain values. In (b)–(e), the model predictions (solid curves) are compared with fully vectorial calculations (circles). For the sake of clarity, in (d) and (e), the model predictions are blue-shifted by 20 nm to compensate for the slight offset in $\text{Re}(n_{\text{eff}})$ due to the small metal thickness; see (b).

with g; see Fig. 3(a). Note that gain negligibly influences $\text{Re}(n_{\text{sp}})$ but largely affects the characteristic length of the transversal resonance that extends over 30 periods for $g = 0.022$.

We next study the loss-compensated fishnet effective index, which is still given by Eq. (2) in the presence of small gain. As shown in Fig. 4(b), $\text{Re}(n_{\text{eff}})$ is insensitive to the modest gain increase and remains negative. More importantly, the attenuation $\text{Im}(n_{\text{eff}})$ is significantly lowered as g increases; see Fig. 4(c). When the gap-SPP damping is exactly compensated by amplification, i.e., for $\text{Im}(n_{\text{sp}}) \to 0$, the resonance linewidth of $|\gamma|^2$ becomes limited by scattering losses. They can be partly compensated for larger gain because the gap-SPP becomes slightly amplified; see Fig. 4(a). For $g = 0.022$, the fishnet becomes an amplifying medium [$\text{Im}(n_{\text{eff}}) < 0$] for $1.75 < \lambda < 1.8\ \mu$m, as shown by the black curve in Fig. 4(c). We have tested the predictions obtained for the Bloch mode of an infinite fishnet by analyzing a real situation with a finite-thickness fishnet composed of 5 unit cells and illuminated from air at normal incidence. Figures 4(d) and 4(e) compare the specular transmission T and reflection R, obtained either by the Fabry-Perot model (solid curves) assuming that the energy transport through the fishnet slab is solely mediated by the fundamental Bloch mode with an effective index $n_{\text{eff}}(g)$ [9] or by fully vectorial calculations (circles) obtained with the rigorous-coupled-wave analysis. Except for a systematic spectral shift that has been removed and that is due to the slight offset of the model predictions for $\text{Re}(n_{\text{eff}})$ observed in Figs. 4(b) or 2(a), the model is found to be highly accurate despite its simplicity.

In summary, light transport in fishnet NIMs has been analyzed with a comprehensive and accurate model. In addition to providing an analytical treatment, the model shines new light on how a negative index is formed and how the inevitable losses associated to a magneticlike resonance can be compensated by incorporating gain. We have shown that gain mainly affects the attenuation, leaving the negative real part of the refractive index unchanged. However, at the transparency threshold, the transversal SPP resonance becomes delocalized over a few tens of unit cells, and fishnets with gain should not be considered as 3D metamaterials but rather as 1D layered systems. The microscopic formalism that tracks the local transport of electromagnetic fields in the structure is especially suited for metamaterials composed of meshed channels. Perhaps with a weaker analyticity of the treatment, it could, however, be generalized to other geometries based on localized resonance, such as paired nanorods or split rings [1]. We hope that this formalism may be helpful not only to design NIMs but also to engineer complex metallo-dielectric surfaces in general [23].

H. T. Liu acknowledges support from CNRS. We thank Jean-Paul Hugonin for computational assistance.

*christophe.sauvan@institutoptique.fr

[1] V. M. Shalaev, Nat. Photon. **1**, 41 (2007).
[2] C. M. Soukoulis and M. Wegener, Science **330**, 1633 (2010).
[3] S. Zhang *et al.*, Phys. Rev. Lett. **95**, 137404 (2005).
[4] J. Valentine *et al.*, Nature (London) **455**, 376 (2008).
[5] D. Schurig *et al.*, Science **314**, 977 (2006).
[6] D. R. Smith and J. B. Pendry, J. Opt. Soc. Am. B **23**, 391 (2006).
[7] S. Zhang *et al.*, Opt. Express **14**, 6778 (2006).
[8] C. Rockstuhl *et al.*, Phys. Rev. B **78**, 155102 (2008).
[9] J. Yang *et al.*, Appl. Phys. Lett. **97**, 061102 (2010).
[10] J. Petschulat *et al.*, Phys. Rev. A **78**, 043811 (2008).
[11] K. Vynck *et al.*, Phys. Rev. Lett. **102**, 133901 (2009).
[12] D. R. Smith *et al.*, Phys. Rev. B **65**, 195104 (2002).
[13] L. Solymar and E. Shamonina, *Waves in Metamaterials* (Oxford University, New York, 2009).
[14] F. Medina, F. Mesa, and R. Marques, IEEE Trans. Microwave Theory Tech. **56**, 3108 (2008); R. Marques *et al.*, Opt. Express **17**, 11 582 (2009).
[15] S. Xiao *et al.*, Nature (London) **466**, 735 (2010).
[16] A. Fang *et al.*, Phys. Rev. B **79**, 241104(R) (2009).
[17] S. Wuestner *et al.*, Phys. Rev. Lett. **105**, 127401 (2010).
[18] E. Silberstein *et al.*, J. Opt. Soc. Am. A **18**, 2865 (2001); H. T. Liu and P. Lalanne, Nature (London) **452**, 728 (2008).
[19] A. Mary *et al.*, Phys. Rev. Lett. **101**, 103902 (2008).
[20] See Supplemental Material at http://link.aps.org/supplemental/10.1103/PhysRevLett.107.043903 for more details on the derivation of Eqs. (1) and (2).
[21] Note that $\text{Im}(n_h)$ is large because the TE_{01} mode is evanescent below cutoff, whereas scattering losses due to the launching of gap-SPPs into the transversal MIM waveguides are responsible for the large value of $\text{Im}(n_{\text{pc}})$.
[22] J. Zhou *et al.*, Phys. Rev. B **80**, 035109 (2009).
[23] T. S. Kao *et al.*, Phys. Rev. Lett. **106**, 085501 (2011).
[24] E. D. Palik, *Handbook of Optical Constants of Solids* (Academic, New York, 1985).